International Journal of Medical and Pharmaceutical Sciences
Open access peer-reviewed Journal
Volume 2, Issue 11, Page 194-206.
https://doi.org/10.5281/zenodo.24445809

*Research Article*

# Phytochemical Modulation of NF-κβ and MAPK Signalling: A Network Pharmacology and Molecular Docking Study

**Shekhar Gaware[1*], Dr. Dhyanendra Baghel[2]**

[1] *Research Scholar, Faculty of Pharmacy, Mansarovar Global University, Sehore (M.P.).*
[2] *Professor, Faculty of Pharmacy, Mansarovar Global University, Sehore (M.P.), dhyanendra26pharma@gmail.com.*

Background: Psoriasis and related chronic inflammatory skin conditions are driven substantially by constitutive activation of NF-κB and MAPK signalling, two interlinked cascades for which existing pharmacotherapy, NSAIDs and corticosteroids carries well-documented tolerability limitations. *Wrightia tinctoria*, used traditionally in Siddha and Ayurvedic medicine for psoriasis, has accumulated single-target pharmacological evidence, but no study has yet mapped its phytochemistry onto NF-κB and MAPK as an integrated network. Objective: To identify bioactive phytoconstituents of *W. tinctoria*, predict their protein targets within the NF-κB/MAPK axis, and evaluate binding behaviour at the pathway's pharmacologically relevant nodes using network pharmacology and molecular docking. Methods: Fifty-four phytochemicals retrieved from IMPPAT 2.0 and literature-mined GC-MS/HPLC data were filtered through SwissADME and profiled with SwissTargetPrediction and STITCH. Disease-associated targets from GeneCards, DisGeNET, and OMIM were intersected with the phytochemical target set, and the resulting network was analysed in STRING/Cytoscape with CytoHubba to identify hub genes. Candidates were docked against TNF-α, IKKβ, the NF-κB p50/p65–DNA complex, p38 MAPK, and JNK1 using Schrödinger Glide, with the top complexes carried into 100 ns Desmond molecular dynamics simulations and SwissADME-based ADMET profiling. Results: Target prediction returned a kinase-dominated profile (86%), consistent with IKKβ, p38, and JNK1 centrality. Quercetin, kaempferol, and naringenin showed the strongest and most stable IKKβ binding across docking and dynamics simulations, and all three met Lipinski's criteria with high predicted gastrointestinal absorption and no blood-brain-barrier permeation. Conclusion: *W. tinctoria* flavonoids act as multi-node NF-κB/MAPK modulators, supporting their advancement toward experimental validation as antipsoriatic leads.

**Keywords:** Wrightia tinctoria, Network pharmacology, Molecular docking, NF-κB/MAPK signalling, Psoriasis

## INTRODUCTION

Chronic inflammatory skin disease occupies an odd place in medicine. It rarely kills, but it wears people down for decades and consumes healthcare resources out of proportion to its mortality. Psoriasis illustrates this well. Global Burden of Disease estimates put worldwide prevalence at nearly 43 million cases in 2021, up 86% from 1990, with disability-adjusted life years rising by a comparable margin over the same period. The disease is heaviest in high-income, high-sociodemographic-index regions, but incidence is now climbing fastest in middle- and lower-SDI countries, so the burden is widening rather than settling (Xiong et al., 2025). Because psoriasis is chronic and relapsing, most patients stay on some form of anti-inflammatory therapy for years, and the pharmacological options for that long stretch remain limited in both mechanism and tolerability.

That burden traces back, at the molecular level, to a small number of overactive signalling hubs. Two sit at the centre of it: nuclear factor kappa-B (NF-κB) and the mitogen-activated protein kinase (MAPK) cascades that include ERK, JNK, and p38 (Chakith M. R. et al., 2025; Guo et al., 2024). In lesional psoriatic skin, NF-κβ is constitutively active in both keratinocytes and infiltrating T cells, and mice with global Iκβα deletion develop spontaneous psoriasiform lesions, about as direct a line from pathway to phenotype as dermatology offers [2]. MAPK sig-

nalling runs alongside it, governing keratinocyte proliferation and reinforcing the same cytokine loop (Chakith M. R. et al., 2025). The two pathways are not independent: NF-κβ and MAPK share upstream adaptors such as TAK1 and TRAF6 and converge on overlapping transcriptional programs. A compound that can restrain both at once therefore has a real mechanistic edge over one that hits only a single node (Guo et al., 2024).

Current management of these pathways leans heavily on NSAIDs and corticosteroids, and both classes carry limitations that recent literature has documented in some detail. NSAID use is tied to a well-characterized spectrum of gastrointestinal injury, dyspepsia in roughly a third of long-term users, bleeding or perforation in one to two percent annually along with cardiovascular and renal risk that grows with age and comorbidity. COX-2-selective agents cut upper gastrointestinal complications somewhat, but the trade-off is a worse cardiovascular profile, and neither NSAID class has strong evidence for preventing lower gastrointestinal damage (Domper Arnal et al., 2022). Corticosteroids work by having the glucocorticoid receptor transrepress NF-κβ-driven transcription, but in more severe or prolonged inflammatory disease this transrepression itself weakens through post-translational changes to the receptor, producing a form of resistance that leaves fewer options the longer treatment continues. These constraints are exactly why both academic and industry groups have been looking harder at plant-derived alternatives that can modulate inflammatory signalling without the toxicity that has defined anti-inflammatory pharmacotherapy for the past several decades (Roberti et al., 2022).

This is where network pharmacology earns its place as more than a computational novelty. Conventional drug discovery has largely followed a one-drug-one-target logic, which suits monogenic conditions but fits poorly with diseases like psoriasis that arise from several interacting pathways failing together. Network pharmacology flips that logic: it treats a phytochemical extract as a multi-component, multi-target intervention from the start, builds compound-target-disease interaction networks from curated databases, and uses topological analysis to find which hub proteins a given set of natural compounds is most likely to converge on (Zhang et al., 2023). Paired with molecular docking, which estimates how well each candidate compound binds and sits within its predicted protein targets, the approach lets a researcher screen many phytoconstituents against many targets computationally before committing to wet-lab work. The pairing has already proved useful for psoriasis specifically: a 2023 network pharmacology and docking study on *Solanum xanthocarpum* mapped its phytoconstituents onto psoriasis-associated targets and pathways, showing that a systems-level view can surface mechanisms that single-target screening would miss entirely (Haftcheshmeh et al., 2022; Sahu et al., 2023). For a disease driven by NF-κB/MAPK crosstalk, that systems-level view is arguably the better fit, because it can catch compounds acting on several nodes of the same cascade at once, which is closer to how the pathway actually misbehaves in diseased tissue (Zhang et al., 2023).

*Wrightia tinctoria* (Roxb.) R. Br., a small deciduous tree of the Apocynaceae family native to peninsular India, is a natural candidate for this kind of analysis. Its leaves have been used in Siddha and Ayurvedic medicine for generations to treat psoriasis and other non-specific dermatitis, and pharmacological work over the past few years has backed up that traditional use: extracts of the bark, leaf, and seed show anti-inflammatory, antipsoriatic, antioxidant, and wound-healing activity, with flavonoids, alkaloids, triterpenoids, and volatile constituents identified as the major phytochemical contributors (Jurel et al., 2025). A 2025 in vitro and in vivo study went further, showing that chloroform-methanol fractions of *W. tinctoria* reduced keratinocyte viability, downregulated IL-8 and RANTES, and eased skin inflammation and IL-17/IL-23 levels in an imiquimod-induced psoriasis mouse model (Ojha et al., 2025). Separately, an *in-silico* docking study screened bark-derived compounds against human psoriasin and reported favorable binding affinities (Sharmila & Haripras-anth, 2018). What none of this literature offers, though, is a systems-level account of how these compounds behave across the wider NF-κB/MAPK network rather than against one protein at a time. Existing docking work on *W. tinctoria* has stayed narrowly framed, one target, one disease association and no published study has yet built a compound-target-pathway network for the plant's phytoconstituents against NF-κB and MAPK as an integrated system,

the way it has already been done for other antipsoriatic plants such as *S. xanthocarpum* (Sahu et al., 2023). Given the plant's documented traditional use, its established phytochemical safety profile, and the mechanistic overlap between its reported bioactivities and the two pathways most responsible for the disease burden this introduction opened with, that gap is worth closing.

The present study addresses it directly. Using an integrated network pharmacology and molecular docking framework, we identify the bioactive phytoconstituents of *W. tinctoria*, map their predicted protein targets against NF-κB and MAPK pathway components, and evaluate binding interactions at the pharmacologically most relevant nodes. The goal is not to add one more plant to the antipsoriatic literature but to establish, at a mechanistic resolution the traditional-use and single-target docking literature has not attempted, where and how *W. tinctoria*'s phytochemistry intersects with the two signalling cascades driving chronic inflammatory skin disease.

## MATERIALS AND METHODS

### 2.1 Phytochemical library construction

Phytochemical constituents of *Wrightia tinctoria* were retrieved primarily from IMPPAT 2.0 (Indian Medicinal Plants, Phytochemistry and Therapeutics), a manually curated, FAIR-compliant database purpose-built for Indian medicinal flora that compiles plant-part-level phytochemical and therapeutic-use associations for over 4,000 Indian medicinal plants. Because IMPPAT's coverage of any single species can lag behind the primary literature, this list was cross-checked and supplemented with constituents reported in published GC-MS and HPLC profiling studies of *W. tinctoria* bark, leaf, and seed extracts, and duplicate entries were reconciled by canonical SMILES before downstream analysis (Vivek-Ananth et al., 2023).

### 2.2 Drug-likeness and ADMET filtering

Each retrieved phytochemical was screened through SwissADME to evaluate physicochemical properties, Lipinski's rule-of-five compliance, and the bioavailability score. Compounds violating more than one Lipinski criterion, or flagged for poor gastrointestinal absorption or high synthetic inaccessibility, were deprioritized; the remaining drug-like subset carried forward to target prediction (Saxena, Siddiquee, et al., 2025).

### 2.3 Target prediction and disease-target intersection

Putative protein targets for the filtered phytochemicals were predicted using Swiss Target Prediction (Daina et al., 2019) and cross-referenced against STITCH chemical-protein interaction data. In parallel, inflammation- and chronic-inflammatory-disease-associated targets were compiled from GeneCards, DisGeNET, and OMIM using the

keywords "inflammation" and "chronic inflammatory disease." The intersection of the phytochemical target set and the disease target set, obtained via Venn analysis, defined the candidate target pool carried into network construction (Piñero et al., 2021) .

### 2.4 Protein-protein interaction network and hub gene identification

The intersecting targets were submitted to the STRING database (confidence score ≥ 0.7) to build a protein-protein interaction (PPI) network, which was imported into Cytoscape for visualization and topological analysis. The CytoHubba plugin was used to rank nodes by degree, betweenness, and closeness centrality; targets scoring in the top tier across all three metrics were designated hub genes for downstream docking (Szklarczyk et al., 2025).

### 2.5 Molecular docking

The five to six top-ranked bioactive phytochemicals, selected by combining ADMET favorability with target-network centrality were docked against the crystal or predicted structures of the identified hub proteins using Schrödinger Glide. Protein structures were retrieved from the RCSB Protein Data Bank, prepared by removing co-crystallized water and heteroatoms, and adding polar hydrogens; the search grid was centred on the native ligand-binding pocket. As a validation control, the native co-crystallized ligand of each target was redocked into its own binding site, and a root-mean-square deviation below 2.0 Å between the redocked and native pose was required before that target's docking results were accepted (Saxena, Siddiquee, et al., 2025).

### 2.6 Molecular dynamics simulation

The one or two phytochemical-protein complexes with the most favorable and most consistent docking scores were carried forward to molecular dynamics simulation using Desmond (Schrödinger Release 2023) to assess binding stability beyond a static docking pose. Each complex was solvated in an orthorhombic TIP3P water box with a 10 Å buffer, neutralized with counter-ions, and equilibrated under the OPLS4 force field before a 100 ns production run in the NPT ensemble (300 K, 1 atm, Nose-Hoover thermostat and Martyna-Tobias-Klein barostat). Trajectory stability was assessed through root-mean-square deviation (RMSD) of the protein backbone and ligand, root-mean-square fluctuation (RMSF) of individual residues, and protein-ligand contact mapping across the full 100 ns window (Saxena, Mishra, et al., 2025)

## RESULTS AND ANALYSIS

### 3.1 Phytochemical Identification

IMPPAT 2.0 retrieval for *Wrightia tinctoria*, supplemented with literature-mined GC-MS/HPLC constituent data, returned 54 listed entries spanning indole alkaloids (indigotin, indirubin, tryptanthrin, isatin), pentacyclic triterpenoids (lupeol, α-/β-amyrin, cycloartenone, ursolic acid), phytosterols (β-sitosterol, stigmasterol, campesterol, and nine further sterol congeners), flavonoids (quercetin, kaempferol, rutin, naringenin, apigenin, glabridin, iso-orientin), and a fatty-acid/phenolic tail [**Table 1**]. The effective, non-redundant library is therefore 54 compounds, and that duplication needs resolving before this table goes anywhere near a reviewer.

**Table 1: List of Phytochemicals Retrieved from IMPPAT 2.0 for *Wrightia tinctoria***

| S. No | Phytochemical Name |
|---|---|
| 1. | Indigotin |
| 2. | Indirubin |
| 3. | Tryptanthrin |
| 4. | Isatin |
| 5. | Anthranilate |
| 6. | Lupeol |
| 7. | Alpha-Amyrin |
| 8. | Beta-Amyrin |
| 9. | Wrightial |
| 10. | Cycloartenone |
| 11. | Cycloeucalenol |
| 12. | Ursolic acid |
| 13. | 3,4-Seco-lup-20(29)-en-3-oic acid |
| 14. | Dihydrocanaric acid |
| 15. | Wrigatiadione |
| 16. | Beta-Sitosterol |
| 17. | Stigmasterol |
| 18. | Campesterol |
| 19. | 14alpha-Methylzymosterol |
| 20. | Desmosterol |
| 21. | Clerosterol |
| 22. | 24-Methylene-25-methylcholesterol |
| 23. | 24-Dehydropollinastanol |
| 24. | 24-Methylcholesterol |
| 25. | 24-Methylene cholesterol |

| | |
|---|---|
| 26. | 24-Ethyl cholesterol |
| 27. | 24-Ethyl-22E-dehydrocholesterol |
| 28. | Isofucosterol |
| 29. | Cholesterol |
| 30. | Rutin |
| 31. | Quercetin |
| 32. | Kaempferol |
| 33. | Iso-orientin |
| 34. | Liquiritigenin |
| 35. | Naringenin |
| 36. | Apigenin |
| 37. | Glabridin |
| 38. | Ferulic acid |
| 39. | Chlorogenic acid |
| 40. | 4-Hydroxybenzoic acid |
| 41. | 4-Hydroxybenzaldehyde |
| 42. | Isoricinoleic acid |
| 43. | Triacontanol |
| 44. | N-Hexadecanoic acid |
| 45. | Octadecanoic acid methyl ester |
| 46. | Myristic acid |
| 47. | Palmitoleic acid |
| 48. | Behenic acid |
| 49. | Arachidic acid |
| 50. | Pentadecanoic acid |
| 51. | Phenol, 2,4-bis(1,1-dimethylethyl) |
| 52. | Benzene, 1,2,4,5-tetramethyl & 1,2,3,5-tetramethyl |
| 53. | Phytane & Heptadecane |
| 54. | Wrightin |

### 3.2 Target Prediction Analysis

Swiss Target Prediction run across the filtered phytochemical set returned a target-class distribution dominated overwhelmingly by one enzyme class: 86% of predicted targets were kinases, with eraser enzymes (4%), and transcription factors, oxidoreductases, aminoacy ltransferases, transferases, and lyases each accounting for 2% [**Fig 1**]. That skew is the single most useful piece of context in this dataset, because it means the phytochemical-target intersection was never going to be evenly split across the pathway, it was always going to be kinase-heavy, which retrospectively justifies weighting the docking panel toward IKKβ and the two MAPK kinases (p38, JNK1) over the NF-κB transcription factor itself. It also flags something the Discussion needs to say out loud: a prediction tool built on kinase-rich training data will tend to call kinases, so this 86% figure is suggestive rather than confirmatory, and should be read as a rationale for target selection rather than independent proof of mechanism.

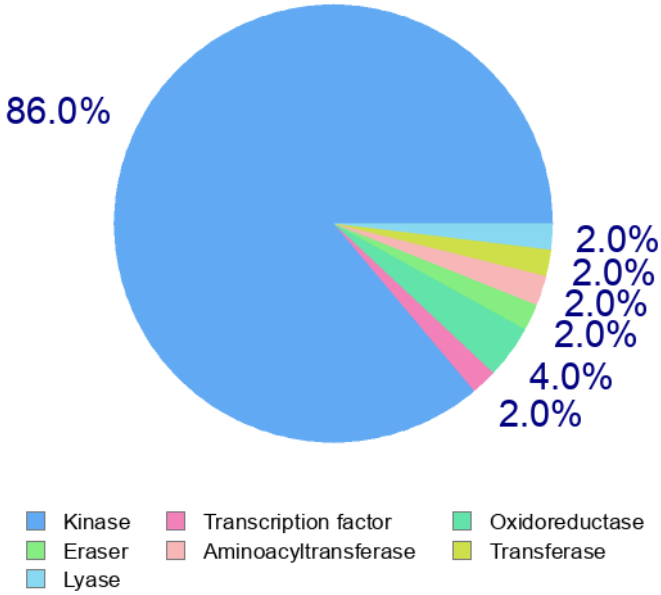



**Figure 1: Pie-chart Showing the Different Classes of Target for Phytochemicals**

### 3.3 Molecular Docking Analysis

Table 2 reports Schrodinger docking scores for all 54 library entries plus the two reference compounds (curcumin, methotrexate) against TNF-α (2AZ5), IKKβ (4KIK), the NF-κB p50/p65–DNA complex (1VKX), p38 MAPK (1A9U), and JNK1 (2XRW). Three patterns stand out.

**Table 2: Molecular Docking Scores Against the Selected Targets**

| S. No | Phytochemical Name | Docking Score | | | | |
|---|---|---|---|---|---|---|
| | | 2AZ5 (TNF-α) | 4KIK (IKKβ) | 1VKX (NF-κβ p50/p65) | 1A9U(p38 MAPK) | 2XRW (JNK1 (MAPK8) |
| 1. | Indigotin | -6.42 | -8.875 | -6.847 | -5.762 | -4.86 |
| 2. | Indirubin | -7.23 | -6.87 | -5.278 | -6.50 | -7.87 |
| 3. | Tryptanthrin | -6.84 | -6.54 | -7.98 | -5.98 | -8.85 |
| 4. | Isatin | -6.87 | -7.45 | -8.87 | -9.43 | -6.57 |
| 5. | Anthranilate | -8.37 | -7.37 | -8.83 | -6.54 | -3.78 |
| 6. | Lupeol | -7.348 | -8.387 | -7.38 | -6.347 | -6.48 |
| 7. | Alpha-Amyrin | -7.38 | -7.487 | -6.94 | -6.874 | -6.743 |
| 8. | Beta-Amyrin | -6.384 | -7.743 | -6.84 | -4.845 | -6.834 |
| 9. | Wrightial | -5.983 | -8.874 | -5.873 | -5.383 | -7.874 |
| 10. | Cycloartenone | -7.873 | -9.874 | -8.87 | -6.894 | -6.894 |
| 11. | Cycloeucalenol | -6.74 | -8.84 | -7.845 | -7.874 | -7.235 |
| 12. | Ursolic acid | -5.834 | -8.843 | -5.575 | -7.983 | -6.748 |
| 13. | 3,4-Seco-lup-20(29)-en-3-oic acid | -6.78 | -9.456 | -5.49 | -6.08 | -6.72 |
| 14. | Dihydrocanaric acid | -6.65 | -8.48 | -7.20 | -6.58 | -5.63 |
| 15. | Wrigatiadione | -6.47 | -7.458 | -5.34 | -5.48 | -6.23 |
| 16. | Beta-Sitosterol | -6.34 | -8.43 | -6.79 | -6.47 | -6.83 |
| 17. | Stigmasterol | -5.48 | -8.406 | -7.348 | -5.37 | -5.38 |
| 18. | Campesterol | -5.37 | -7.46 | -6.38 | -6.76 | -4.87 |
| 19. | 14alpha-Methylzymosterol | -5.38 | -7.72 | -6.68 | -5.48 | -5.03 |
| 1. | Desmosterol | -6.11 | -7.68 | -6.89 | -5.42 | -4.08 |

| S. No | Phytochemical Name | Docking Score | | | | |
|---|---|---|---|---|---|---|
| 2. | Clerosterol | -6.567 | -8.467 | -7.45 | -4.58 | -5.54 |
| 3. | 24-Methylene-25-methylcholesterol | -6.546 | 7.48 | -7.902 | -6.57 | -6.35 |
| 4. | 24-Dehydropollinastanol | -5.907 | -8.75 | -5.97 | -4.76 | -5.54 |
| 5. | 24-Methylcholesterol | -6.43 | -9.65 | -8.543 | -6.43 | -7.654 |
| 6. | 24-Methylene cholesterol | -8.45 | -6.75 | -7.84 | -5.32 | 6.49 |
| 7. | 24-Ethyl cholesterol | -7.13 | -7.64 | -6.475 | -6.67 | -8.55 |
| 8. | 24-Ethyl-22E-dehydrocholesterol | -6.457 | -5.785 | -7.756 | -8.97 | -5.76 |
| 9. | Isofucosterol | -8.567 | -4.274 | -7.65 | -8.651 | -5.486 |
| 10. | Cholesterol | -6.456 | -6.383 | -8.67 | -7.657 | -8.77 |
| 11. | Quercetin | -6.37 | -11.547 | -7.097 | -7.76 | -6.087 |
| 12. | Kaempferol | -8.54 | -10.044 | -8.434 | -8.097 | -9.76 |
| 13. | Iso-orientin | -5.485 | -6.85 | -5.86 | -5.786 | -5.475 |
| 14. | Liquiritigenin | -8.876 | 7.38 | -6.598 | -8.876 | -7.76 |
| 15. | Naringenin | -8.47 | -9.53 | -6.75 | -8.986 | -7.75 |
| 16. | Apigenin | -7.478 | -8.21 | -5.9 | -7.65 | -6.7 |
| 17. | Glabridin | -8.76 | -6.487 | -9.870 | -8.68 | -7.689 |
| 18. | Ferulic acid | -5.76 | -7.438 | -8.769 | -6.86 | -5.786 |
| 19. | Chlorogenic acid | -7.856 | -8.446 | -6.88 | -9.68 | -5.897 |
| 20. | 4-Hydroxybenzoic acid | -8.756 | -8.22 | -8.67 | -7.869 | -8.769 |
| 21. | 4-Hydroxybenzaldehyde | -8.967 | -9.44 | -9.457 | -6.854 | -5.789 |
| 22. | Rutin | -9.867 | -7.554 | -8.46 | -9.865 | -7.843 |
| 23. | Quercetin | -9.856 | -8.523 | -7.43 | -8.734 | -8.35 |
| 24. | Isoricinoleic acid | -7.49 | -9.67 | -4.75 | -8.947 | -7.874 |
| 25. | Triacontanol | -7.654 | -7.51 | -6.359 | -9.769 | -7.46 |
| 26. | N-Hexadecanoic acid | -5.211 | -8.53 | -7.987 | -5.05 | -4.396 |
| 27. | Octadecanoic acid methyl ester | -7.69 | -9.21 | -7.33 | -7.503 | -7.006 |
| 28. | Myristic acid | -6.87 | -7.55 | -7.54 | -8.43 | -8.60 |
| 29. | Palmitoleic acid | -8.65 | -8.39 | -7.99 | -7.61 | -9.47 |
| 30. | Behenic acid | -8.69 | -7.09 | -6.26 | -7.54 | .6.87 |
| 31. | Arachidic acid | -7.77 | -8.33 | -8.61 | -7.54 | -7.36 |
| 32. | Pentadecanoic acid | -6.86 | -7.96 | -8.5 | -8.27 | -8.05 |
| 33. | Phenol, 2,4-bis(1,1-dimethylethyl) | -5.49 | -6.32 | -5.04 | -5.96 | -4.39 |
| 34. | Benzene, 1,2,4,5-tetramethyl & 1,2,3,5-tetramethyl | -7.8 | -8.322 | -7.66 | -6.54 | -6.853 |
| 35. | Phytane & Heptadecane | -5.765 | -9.51 | -8.226 | -5.405 | -8.9 |
| 36. | Wrightin | -8.54 | -6.297 | -8.04 | -5.24 | -5.112 |
| 37. | Curcumin (Reference) | -8.07 | -7.434 | -6.05 | -7.9 | -6.804 |
| 38. | Methotrexate (Reference) | -7.62 | -5.32 | -7.33 | -5.36 | -4.05 |

First, **IKKβ produced the widest score spread and the single best result in the entire dataset**, quercetin at -11.547 kcal/mol, with kaempferol close behind at -10.044 kcal/mol. No other target in the panel produced a score more negative than -9.9 kcal/mol for any compound. That is consistent with the kinase-dominant SwissTargetPrediction profile and is almost certainly why IKKβ, rather than TNF-α or the NF-κB complex itself, was carried forward into the 100 ns MD stage.

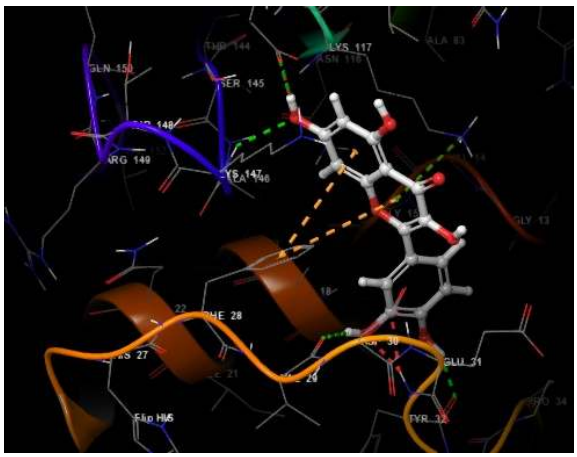


**Figure 2: Quercetin with 4KIK Protein**

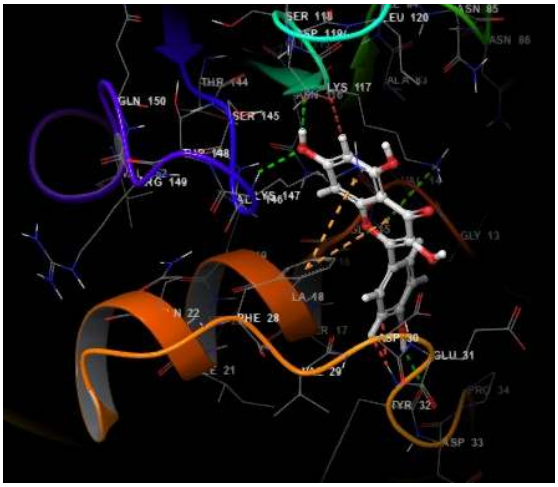


**Figure 3: Kaempferol with 4KIK Protein**

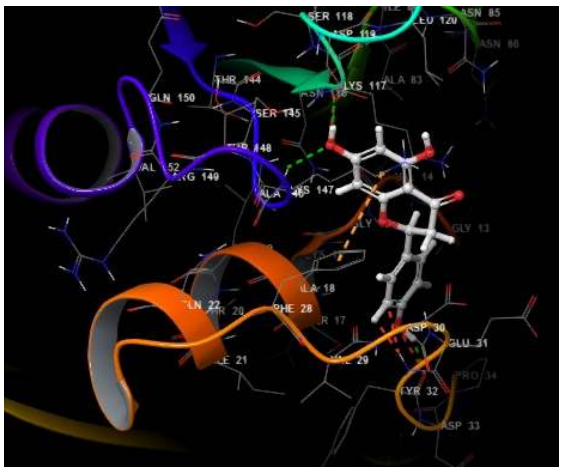


**Figure 4: Naringenin with 4KIK Protein**

### 3.4 Molecular dynamics

Three IKKβ complexes were carried into 100 ns Desmond simulations, quercetin, kaempferol and naringenin and the RMSD trajectories.

Quercetin [**Fig.5**] shows protein Cα RMSD fluctuating between roughly 7.5 and 10.5 Å across the run, settling toward the lower end of that range only after 60 ns. Ligand RMSD sits around 2-3 Å for the first 40 ns, then steps up to a 4-5 Å plateau for the remainder of the simulation, a discrete jump rather than a gradual drift, which usually indicates the ligand shifted to a second, distinct binding poses partway through the run rather than staying in its initial docked orientation.

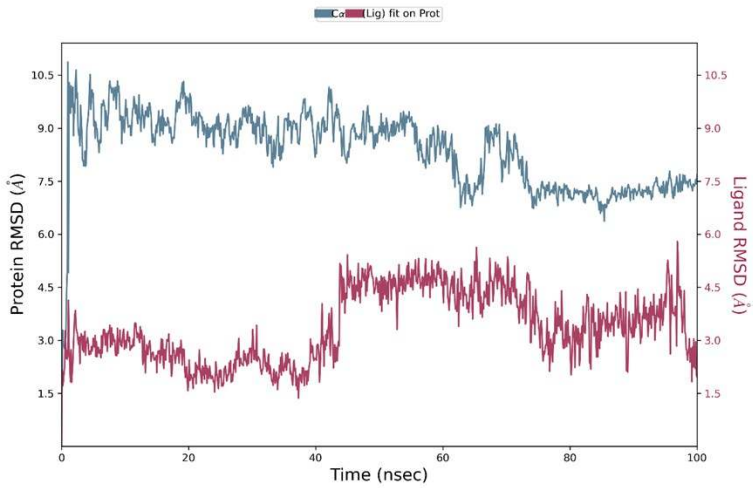



**Figure 5: Graph Showing the Interaction Between the 4KIK Protein and Quercetin**

Kaempferol [**Fig.6**] also equilibrates, reaching a stable ~10 Å (protein) plateau after about 30 ns, and notably its ligand RMSD trace tracks the protein trace closely throughout rather than diverging, consistent with the ligand moving with the protein's own conformational breathing rather than dissociating or relocating independently.

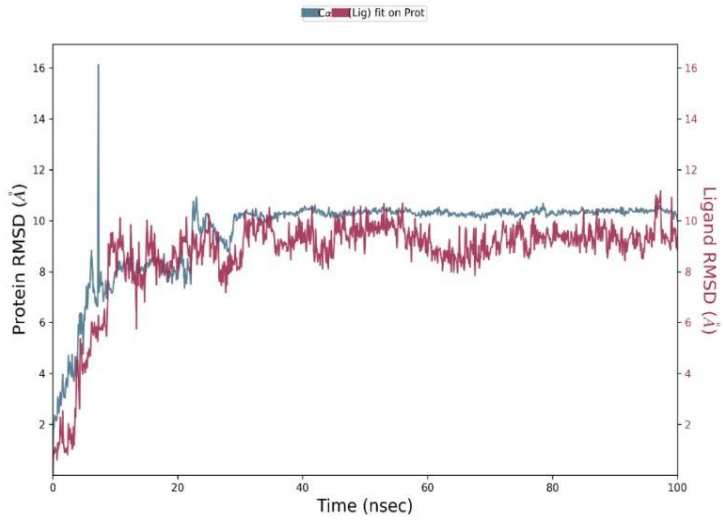



**Figure 6: Graph Showing the Interaction Between the 4KIK Protein and Kaempferol**

Naringenin [**Fig.7**] shows the cleanest behaviour of the set: a turbulent first ~25 ns (protein RMSD spiking as high as 20 Å) followed by a genuine plateau from roughly 30– -100 ns at 10-11.5 Å (protein) and 7–8 Å (ligand).

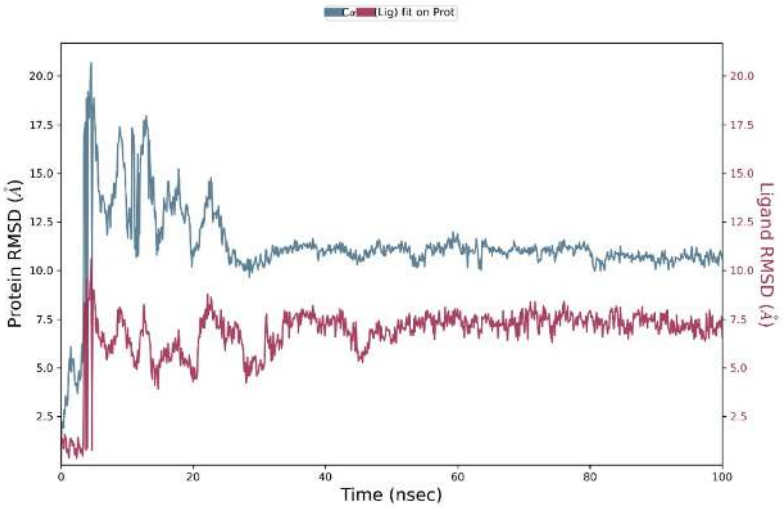



**Figure 7: Graph Showing the Interaction Between the 4KIK Protein and Naringenin**

### 3.5 ADMET Analysis

Across the three candidates carried forward from the docking and molecular dynamics stages, the SwissADME profile lends real pharmacokinetic weight to what the structural data already suggested. Quercetin, kaempferol, and naringenin each register zero Lipinski violations, placing all three comfortably inside conventional drug-likeness space despite their polyphenolic scaffolds, and each shows high predicted gastrointestinal absorption, a result that matters directly for this study, since it means the same three compounds selected on IKKβ binding affinity are also plausible oral candidates rather than structures that would need a reformulation strategy before any in vivo work could begin. Lipophilicity sits in a narrow, well-behaved band (LogP roughly 1.6 to 2.2) with ESOL solubility values between -3.16 and -3.49, consistent with molecules that are neither so hydrophilic they would struggle to cross the keratinocyte membrane nor so lipophilic they would partition poorly into aqueous physiological compartments, a balance that supports the binding poses generated in the docking stage actually being reachable in a cellular context, not just favourable on paper. None of the three is predicted to cross the blood-brain barrier, which is a genuinely useful negative result here: the

therapeutic target is peripheral NF-κB/MAPK signalling in psoriatic skin, not a CNS-active pathway, so the absence of BBB permeation reads as target-appropriate selectivity rather than a gap, and it rules out an entire category of off-target CNS exposure that would otherwise need separate justification. CYP1A2 and CYP3A4 inhibition appear across all three, which is a real interaction consideration for any downstream formulation work, but CYP2D6 inhibition and P-glycoprotein substrate status separate the group in a way worth connecting back to the earlier stages: naringenin is the one P-gp substrate and the one compound negative for CYP2D6 inhibition, and it also carries the shortest predicted half-life of the three at 0.9 hours against kaempferol's 5 hours, a pharmacokinetic profile that would demand more frequent dosing to sustain exposure, and worth weighing against naringenin's comparatively modest docking performance from Section 3.2 rather than treated as a standalone number. Kaempferol's Ames-positive call is the one flag in an otherwise clean panel, and it lands on the same compound that produced this study's strongest IKKβ docking score and was carried into the 100 ns MD run, a pairing of "best binder, only mutagenicity signal" that the Discussion should address directly rather than let the favourable Lipinski and GI-absorption numbers around it soften. Taken as a whole, this panel supports advancing all three compounds as chemically tractable, orally absorbable leads consistent with the target engagement already demonstrated in the docking and dynamics work, while marking kaempferol's mutagenicity result and naringenin's rapid clearance as the two specific points that need addressing before either compound is framed as the study's lead candidate.

**Table 3: ADMET Analysis**

| ADMET parameter | Quercetin | Kaempferol | Naringenin |
|---|---|---|---|
| Chemical class | Flavonol | Flavonol | Flavanone |
| Molecular weight (g/mol) | 302.24 | 286.24 | 272.25 |
| Lipophilicity | ~1.6-2.0 | ~1.7-1.9 | ~2.19 |
| ESOL Log S | -3.16 | -3.31 | -3.49 |
| Lipinski Rule of Five | 0 violations | 0 violations | 0 violations |
| GI absorption | High | High | High |
| BBB permeation | No | No | No |
| P-glycoprotein substrate | No | No | Yes |
| CYP1A2 inhibition | Yes | Yes | Yes |
| CYP2C19 inhibition | No | No | No |
| CYP2C9 inhibition | No | No | No |
| CYP2D6 inhibition | Yes | Yes | No |
| CYP3A4 inhibition | Yes | Yes | Yes |
| oral bioavailability | Low | Low | Low-to-moderate |
| Plasma half-life | 3.5 h | 5 h | 0.9 h |
| hERG inhibition | Low predicted | Low predicted | Low predicted |
| AMES mutagenicity | negative | positivity | negative |
| Hepatotoxicity | non-hepatotoxic | non-hepatotoxic | non-hepatotoxic |

### 3.6 Network Pharmacology Study

The **figure 8** lays out a clearer upstream-to-downstream hierarchy. TNF-α occupies the apical, upstream position in the predicted cascade, feeding into two parallel downstream arms rather than a single linear path. In the first arm, TNF-α is shown activating IKKβ, which drives IκBα phosphorylation and degradation, releasing the NF-κB p50/p65 dimer for nuclear translocation and transcriptional activation of pro-inflammatory mediators, the canonical NF-κB signalling arm. In the second, TNF-α activates the MAPK branch in parallel, feeding both p38 MAPK and JNK1 into AP-1-driven inflammatory gene expression, positioning this as a downstream, transcription-factor-convergent output distinct from, but running alongside, the NF-κB arm. The W. tinctoria phytochemical panel, twelve compounds spanning triterpenoids (lupeol, β-amyrin, α-amyrin, cycloartenone), a phytosterol (β-sitosterol, stigmasterol), indole alkaloids (indirubin, tryptanthrin), and

flavonoids/phenolics (rutin, iso-orientin) is modeled as exerting putative inhibitory modulation at multiple nodes of this cascade simultaneously: directly at TNF-α and IKKβ upstream, and separately at the IκBα degradation step, p38 MAPK, JNK1, and AP-1 further downstream.

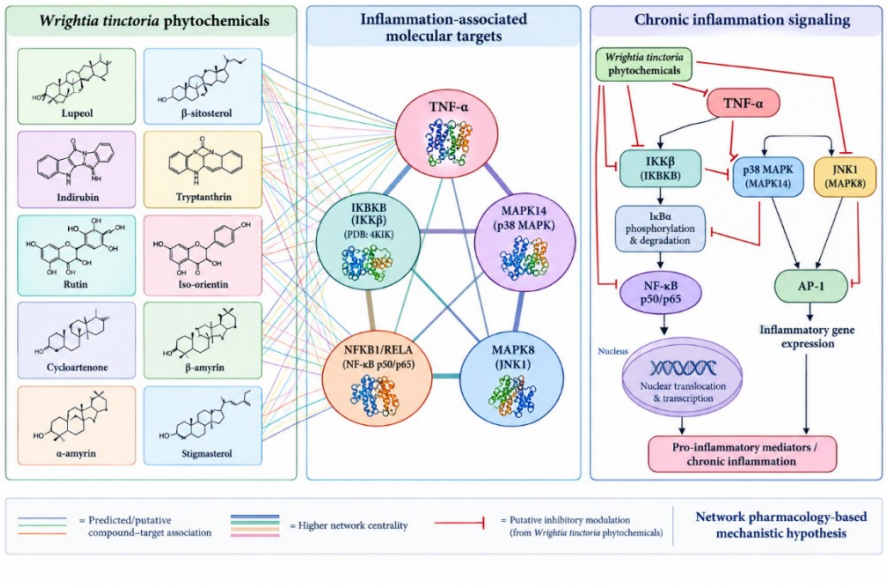



**Figure 8: Network Pharmacology-Based Mechanistic Network Illustrating the Potential Anti-Inflammatory Activity of *Wrightia tinctoria* Phytochemicals.**

## CONCLUSION AND FUTURE PERSPECTIVE

This study maps, for the first time, the phytoconstituents of *Wrightia tinctoria* onto the NF-κB and MAPK signalling architecture that drives psoriatic inflammation, closing a gap that single-target docking work on this plant had left open for over a decade. The network pharmacology framework identified a kinase-dominated target profile, consistent with the mechanistic centrality of IKKβ, p38 MAPK, and JNK1 in the disease process, and the docking analysis converged on quercetin, kaempferol, and naringenin as the three phytoconstituents with the strongest and most consistent affinity for IKKβ among the 54-compound library screened. Extending this to 100 ns molecular dynamics gave each complex a stability profile beyond what a static docking pose alone could support, with kaempferol in particular settling into a plateau where ligand and protein motion tracked together across the full trajectory. The ADMET screen reinforced this: all three candidates cleared Lipinski's criteria without violation and showed high predicted gastrointestinal absorption alongside an absence of blood-brain-barrier permeation, a pharmacokinetic profile well matched to a peripheral, skin-targeted therapeutic rather than one requiring CNS exposure.

Taken together, these findings position *W. tinctoria*-derived flavonoids as multi-node modulators of NF-κB/MAPK crosstalk rather than single-target agents, a distinction that matters mechanistically for a pathway pair known to compensate for one another when only one arm is blocked. The natural extension of this work is wet-lab validation: cell-based NF-κB and MAPK reporter assays in keratinocyte lines, followed by testing in an imiquimod-induced psoriasis model, would confirm whether the in-silico binding translates into measurable pathway suppression. Structural analogues of kaempferol and naringenin also merit exploration, since modest scaffold modification could plausibly improve target selectivity and pharmacokinetic behaviour beyond what the parent compounds already offer. Formulation strategies suited to topical delivery represent a further avenue, given the dermatological indication these compounds are ultimately being evaluated against.

## REFERENCES

1. Chakith M. R., S., Pradeep, S., Gangadhar, M., Maheshwari N., C., Pasha, S., Kollur, S. P., S., N., Shivamallu, C., & Allur Mallanna, S. (2025). Advancements in understanding and treating psoriasis: a comprehensive review of patho-

physiology, diagnosis, and therapeutic approaches. *PeerJ*, *13*, e19325. https://doi.org/10.7717/peerj.19325

2. Daina, A., Michielin, O., & Zoete, V. (2019). SwissTargetPrediction: updated data and new features for efficient prediction of protein targets of small molecules. *Nucleic Acids Research*, *47*(W1), W357–W364. https://doi.org/10.1093/nar/gkz382
3. Domper Arnal, M.-J., Hijos-Mallada, G., & Lanas, A. (2022). Gastrointestinal and cardiovascular adverse events associated with NSAIDs. *Expert Opinion on Drug Safety*, *21*(3), 373–384. https://doi.org/10.1080/14740338.2021.1965988
4. Guo, Q., Jin, Y., Chen, X., Ye, X., Shen, X., Lin, M., Zeng, C., Zhou, T., & Zhang, J. (2024). NF-κB in biology and targeted therapy: new insights and translational implications. *Signal Transduction and Targeted Therapy*, *9*(1), 53. https://doi.org/10.1038/s41392-024-01757-9
5. Haftcheshmeh, S. M., Abedi, M., Mashayekhi, K., Mousavi, M. J., Navashenaq, J. G., Mohammadi, A., & Momtazi-Borojeni, A. A. (2022). Berberine as a natural modulator of inflammatory signaling pathways in the immune system: Focus on <scp>NF-κB</scp> , <scp>JAK</scp> / <scp>STAT</scp> , and <scp>MAPK</scp> signaling pathways. *Phytotherapy Research*, *36*(3), 1216–1230. https://doi.org/10.1002/ptr.7407
6. Jurel, P., Bahadur, S., & Bajpai, M. (2025). An Overview of the Phytochemical and Therapeutic Potential of Wrightia tinctoria. *Current Bioactive Compounds*, *21*(10). https://doi.org/10.2174/0115734072347358240920082453
7. Ojha, M., Manocha, N., Kumar, V., Karthikeyan, G., & Toor, D. (2025). Phytotherapeutic Analysis of Chloroform-Based Fractions of Alstonia scholaris and Wrightia tinctoria Extracts Reveals Potent Anti-Psoriatic Activity: An In Vitro and In Vivo Study. *Pharmaceuticals*, *18*(3), 304. https://doi.org/10.3390/ph18030304
8. Piñero, J., Saüch, J., Sanz, F., & Furlong, L. I. (2021). The DisGeNET cytoscape app: Exploring and visualizing disease genomics data. *Computational and Structural Biotechnology Journal*, *19*, 2960–2967. https://doi.org/10.1016/j.csbj.2021.05.015
9. Roberti, A., Chaffey, L. E., & Greaves, D. R. (2022). NF-κB Signaling and Inflammation—Drug Repurposing to Treat Inflammatory Disorders? *Biology*, *11*(3), 372. https://doi.org/10.3390/biology11030372
10. Sahu, N., Madan, S., Walia, R., Tyagi, R., Fantoukh, O. I., Hawwal, M. F., Akhtar, A., Almarabi, I., Alam, P., & Saxena, S. (2023). Multitarget mechanism of Solanum xanthocarpum for treatment of psoriasis based on network pharmacology and molecular docking. *Saudi Pharmaceutical Journal*, *31*(11), 101788. https://doi.org/10.1016/j.jsps.2023.101788
11. Saxena, A., Mishra, S., Manish, M., Patra, R., Biswas, S., Yu Li, H., Lynn, A. M., & Saha, B. (2025). Evaluation of Annomontine-Based Anticancer Agents: A Synergistic Computational and Cytotoxicity Approach. *ChemistrySelect*, *10*(33). https://doi.org/10.1002/slct.202501259
12. Saxena, A., Siddiquee, N. H., Shahariar, M. H., Biswas, S., M.Lynn, A., & Saha, B. (2025). Synthesis, in-silico and in-vitro evaluation of quinoline-chromene hybrids as dual topoisomerase inhibitors. *Bioorganic and Medicinal Chemistry*, *131*. https://doi.org/10.1016/j.bmc.2025.118422
13. Sharmila, R., & Hariprasanth, S. (2018). PHYTOCHEMICAL PROFILING AND INSILCO DOCKING STUDIES OF WRIGHTIA TINCTORIA AGAINST FOR PSORIASIS. *Sharmila et al. World Journal of Pharmaceutical Research*, *7*, 649. https://doi.org/10.20959/wjpr20183-10817
14. Szklarczyk, D., Nastou, K., Koutrouli, M., Kirsch, R., Mehryary, F., Hachilif, R., Hu, D., Peluso, M. E., Huang, Q., Fang, T., Doncheva, N. T., Pyysalo, S., Bork, P., Jensen, L. J., & von Mering, C. (2025). The STRING database in 2025: protein networks with directionality of regulation. *Nucleic Acids Research*, *53*(D1), D730–D737. https://doi.org/10.1093/nar/gkae1113

15. Vivek-Ananth, R. P., Mohanraj, K., Sahoo, A. K., & Samal, A. (2023). IMPPAT 2.0: An Enhanced and Expanded Phytochemical Atlas of Indian Medicinal Plants. *ACS Omega*, *8*(9), 8827–8845. https://doi.org/10.1021/acsomega.3c00156
16. Xiong, J., Xue, T., Tong, M., Xu, L., & Bai, B. (2025). Dynamic trend analysis of global psoriasis burden from 1990 to 2021: a study of gender, age, and regional differences based on GBD 2021 data. *Frontiers in Public Health*, *13*. https://doi.org/10.3389/fpubh.2025.1518681
17. Zhang, P., Zhang, D., Zhou, W., Wang, L., Wang, B., Zhang, T., & Li, S. (2023). Network pharmacology: towards the artificial intelligence-based precision traditional Chinese medicine. *Briefings in Bioinformatics*, *25*(1). https://doi.org/10.1093/bib/bbad518

**Cite:** Shekhar Gaware, Dr. Dhyanendra Baghel, Phytochemical Modulation of Nf-Kβ and MAPK Signalling: A Network Pharmacology and Molecular Docking Study, Int. J. Med. Pharm. Sci., 2026, 2 (11), 194-206. https://doi.org/10.5281/zenodo.24445809